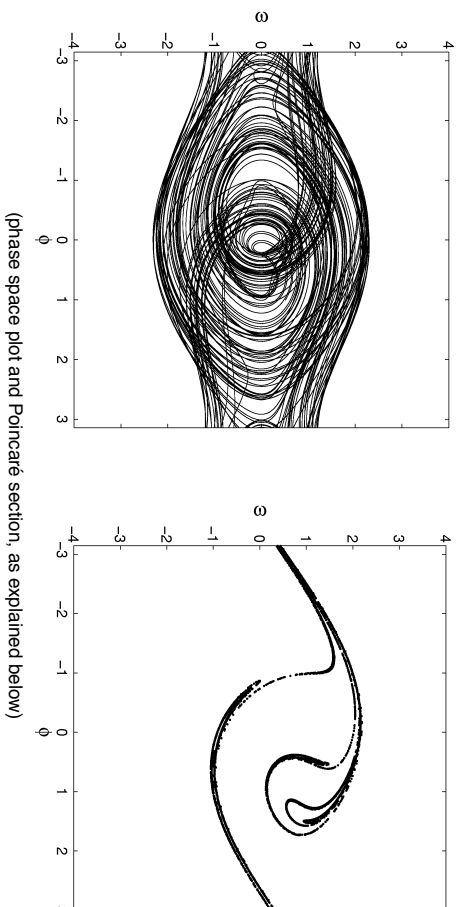




# Chapter I: Nonlinear Maps and Deterministic Chaos

Modelling and Simulation, M. Biehl, 2005

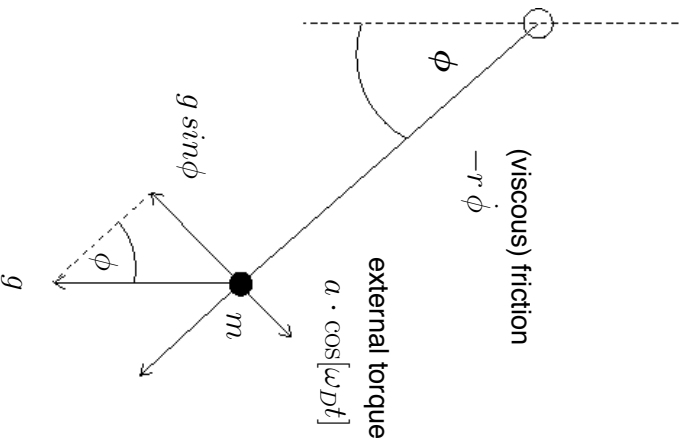
## 3. The driven pendulum



The discussion follows to a large extent the chapter *The Chaotic Pendulum* in W. Kinzel and G. Reents, *Physics by Computer* (Springer, 1998).

Further information and related Mathematica and C programs as well as Java applets are available at <http://theorie.physik.uni-wuerzburg.de/TP3/physbc.html>

RunG



### The driven, damped pendulum:

( we set  $m = g = \ell = 1$  for convenience )

$$\ddot{\phi} = -\sin \phi - r \dot{\phi} + a \cos[\omega_D t]$$

- $\omega_D$  : frequency of the driving torque
- $a$  : amplitude of the driving torque
- $r$  : friction coefficient

rewritten as a system of first order O.D.E. in three dimensions  $\{\phi, \omega, \theta\}$

$$\begin{aligned}\dot{\phi} &= \omega \\ \dot{\omega} &= -\sin \phi - r \omega + a \cos \theta \\ \dot{\theta} &= \omega_D\end{aligned}$$

RunG

## The ideal pendulum

as a test case for numerical integration

$$\begin{aligned}\dot{\phi} &= \omega \\ \dot{\omega} &= -\sin \phi\end{aligned}$$

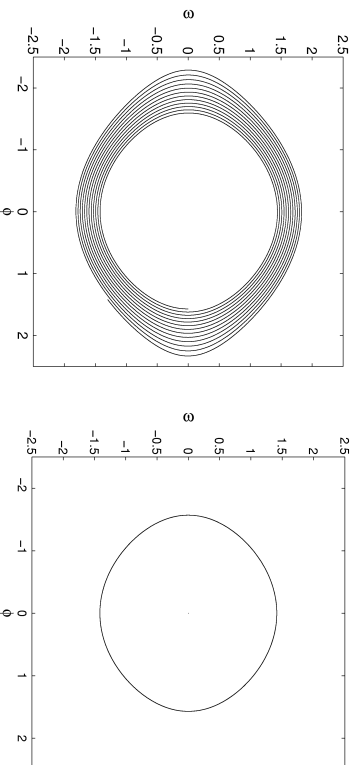


**Fig. 3:** Phase space plot, i.e.  $\omega = \dot{\phi}$  vs.  $\phi$  as obtained for initial conditions  $\phi(0) = \pi/2$  and  $\omega(0) = 0$ .

**Left:** numerical integration with the naive Euler method, time step  $dt = 0.01$ .

**Right:** num. integration with the (Runge Kutta based) Matlab procedure ode45.

For  $a = 0, r = 0$  the total energy is perfectly conserved  $\rightarrow$  initial conditions must be perfectly restored after one period ( $T = 2\pi\sqrt{\ell/g}$  for small  $\phi$ ) Euler integration yields (here) an artificial increase of the energy! (see the discussion in the supplement *Ordinary Differential Equations*)

RunG

## The damped pendulum

without external driving ( $a = 0$ ) and weak damping ( $r < 2$ )

$$\begin{aligned}\dot{\phi} &= \omega \\ \dot{\omega} &= -\sin \phi - r\omega\end{aligned}$$

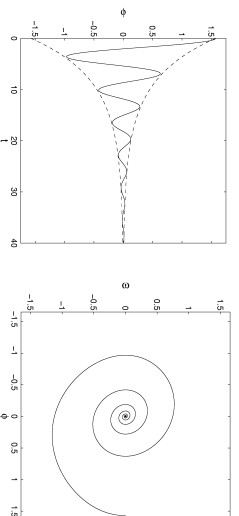


**Fig. 4:** **Left:**  $\phi(t)$  for  $r = 0.25$  and initial conditions  $\phi(0) = \pi/2$  and  $\omega(0) = 0$ . The envelopes are  $\pm \phi(0) \cdot \exp[-rt/2]$  and the frequency is  $\omega_r = (1 - r^2/4)^{1/2}$  for small  $\phi$ .

**Right:** the corresponding phase space plot in the  $(\phi, \omega)$ -plane

From *almost all* initial conditions, the system approaches the stable fixed point  $\phi = 0, \omega = 0$ . The pendulum comes to rest, all energy is dissipated due to friction.

Exception:  $\phi = \pi, \omega = 0$  is an *unstable* fixed point.

**Note:** Trajectories in the phase space plot cannot cross, because the pair  $(\phi, \dot{\phi})$  uniquely determines the further temporal evolution of the system

Closely related statement (yet not obvious):  
**There is no chaotic motion in two-dimensional (continuous) phase space**

RunG

```

function di = dg1(t,y)
% function diff(phi,omega)
% diff. eqs. for the damped, driven pendulum
% phi' = omega, omega' = -r*omega - sin(phi)
% uses GLOBAL variables amp,omd,r
global amp omd r
phi = y(1); omega=y(2); di = zeros(2,1);
di(1) = omega;
di(2) = -r*omega - sin(phi) + amp*cos(omd*t);

function pend(ampin,tmax,all)
% pend(amp,tmax,all)
% fixed: omd=2/3, r=1/4
% all=1: 0<t<tmax, only phase space plot
% all=0: 300 pi<t<tmax, addt1. Poincare section
if (nargin==2) all=0; end
% default accuracy of ode45 is not sufficient!
op = odeset('RelTol',1.e-8);

clear global amp omd r
global amp omd r
amp=ampin; omd=2/3; r=0.25; pd=2*pi/omd;
% initial conditions (horizontal pendulum)
phi0 = pi/2.; om0=0;

if all == 0
% initial phase not plotted
% t is multiple of 2 Pi/omd as to guarantee
% correct initial value of omd*t later
[T,Y] = ode45(@dg1,[0 100*pd],[phi0 om0],op);
lst = length(Y(:,1));

```

```

phi0 = Y(lst,1); om0 = Y(lst,2);
end
close all; figure(1); hold on; box on;
axis square; axis([-pi pi -4 4]);

% integration and phase space plot up to tmax, plot
% phi-intervals [-pi pi],[pi 3pi],... on top of e.a.
[T,Y]=ode45(@dg1,[0 tmax],[phi0 om0],op);
for i=ceil(min(Y(:,1))/2./pi):ceil(max(Y(:,1))/2./pi)
plot(Y(:,1) - i*2*pi, Y(:,2));
end
hold off;

% the Poincare section after initial integration
if all==0
figure(2); hold on; box on;
axis([-pi pi -4 4]); axis square;

% first period and dot plotted
[T,Y] = ode45(@dg1,[0 pd],[phi0 om0],op);
lst = length(Y(:,1));
plot(mod(Y(lst,1)+pi,2*pi)-pi, Y(lst,2),'k.');
```

RunG

## The driven, damped pendulum

three-dim. phase space, or explicit  $t$ -dep.:

$$\begin{aligned}\dot{\phi} &= \omega \\ \dot{\omega} &= -\sin\phi - r\omega + a\cos[\omega D t]\end{aligned}$$

consider in the following:  $r = 0.25$ ,  $\omega D = 2/3$ ,  $\phi(0) = \pi/2$ ,  $\omega(0) = 0$

generic behavior for small driving force:

the driving can compensate the friction; after a more or less complex initial phase, the system approaches an *attractor*, i.e. a periodic state

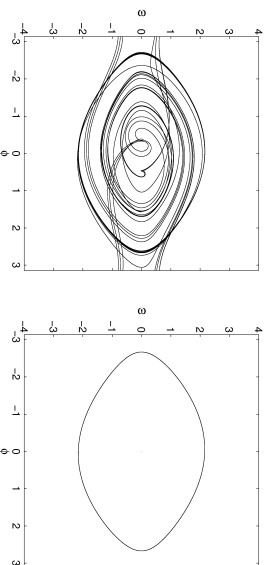


**Fig. 5:** Phase space plot  $\omega$  vs.  $\phi$  for driving force amplitude  $a = 0.6$  in the time interval  $[0, 1000]$  including the initial phase (left) and for the stationary oscillation only (right).

RunG

## The Poincaré section

In order to visualize the behavior in three-dimensional phase space  $(\phi, \omega = \dot{\phi}, \theta = \omega_D t)$ , we make *stroboscopic* snapshots of the position in  $(\phi, \omega)$  after the initial phase  $[0, t_{init}]$

at times  $t_{init} + \frac{2\pi j}{\omega_D}$ ,  $j = 0, 1, 2, \dots$  (multiples of the period  $T_D = 2\pi/\omega_D$ ),  
i.e. for  $\omega_D = 2/3$ :  $t_{init} + 0, 3\pi, 6\pi, \dots$

Poincaré sections display the intersection of the three-dim. trajectories with equidistant planes of constant  $\theta = \omega_D t$

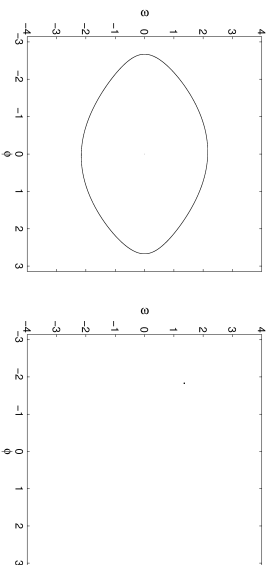


**Fig. 6:** Stationary attractor in  $(\phi, \omega)$  for driving force amplitude  $a = 0.6$  (left, same as above) and the corresponding Poincaré section (right), where the motion is represented by a single dot (exact position depends on  $t_{init}$ ).

For small amplitude  $a$  of the driving torque, we observe a simple periodic movement with frequency  $\omega_D$  as imposed by the external force

RunG

## More complex behavior

- periodic with  $2\pi/\omega_D$ , pendulum turns over once per cycle

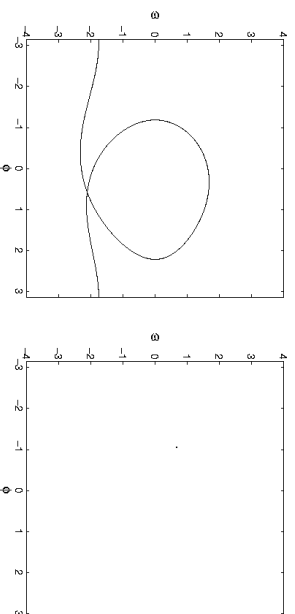


**Fig. 7:**  
Attractor and Poincaré section  
for  $a = 0.97$

- periods  $n \cdot 2\pi/\omega_D$ , e.g.  $n = 2$

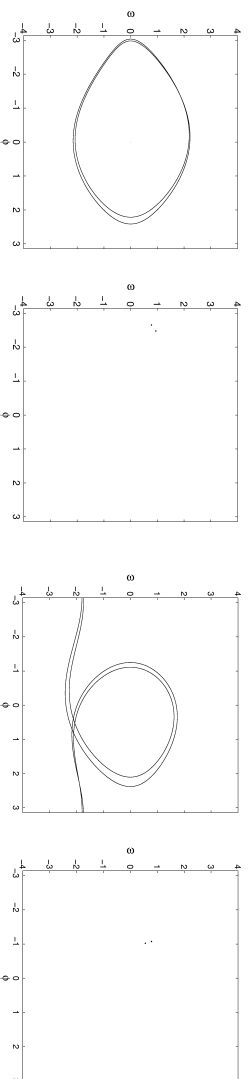


**Fig. 8:** Attractor and Poincaré section for  $a = 0.665$  (left) and  $a = 0.98$  (right)

RunG

- multiple periods, e.g.  $n = 4$  and  $n = 7$

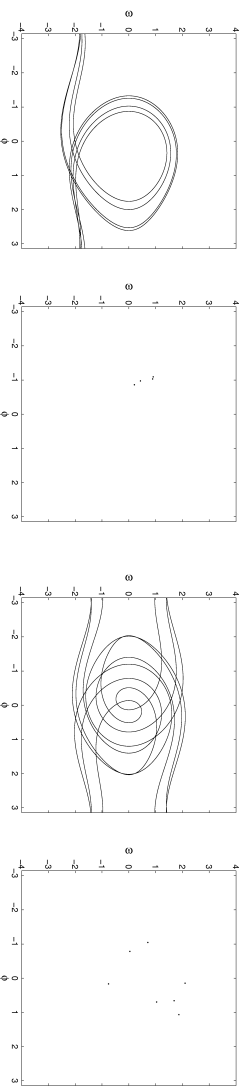


**Fig. 9:** Attractor and Poincaré section for  $\alpha = 1.0$  (left) and  $\alpha = 0.85$  (right)

Note: we can observe period doubling, e.g. for  $\alpha = 0.97, 0.98, 1.0$

- Chaotic behavior

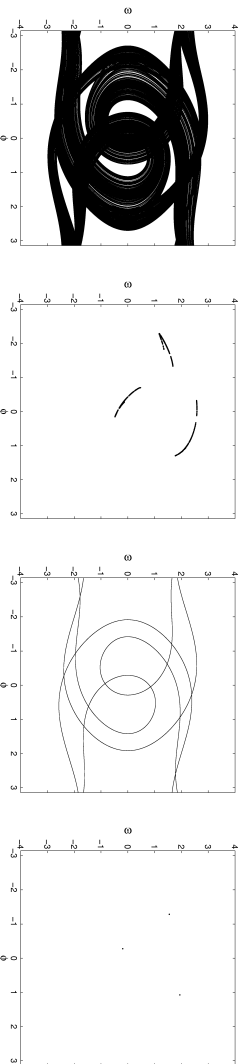


**Fig. 10:** Chaotic behavior at  $\alpha = 1.3$  (left) displays three bands in the Poincaré section. It is reminiscent of the  $n = 3$  periodic state for  $\alpha = 1.2$  (right)

RunG

- Strange attractors

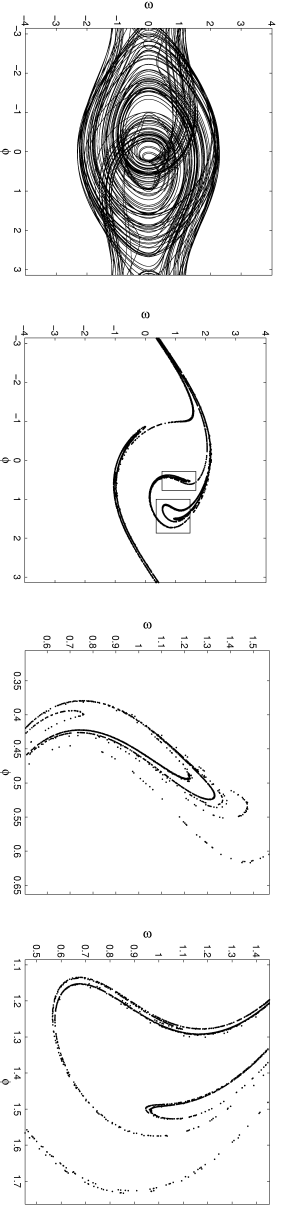


**Fig. 11:**

**Left:** phase space plot for  $\alpha = 0.7$ , here the integration was up to  $t_{max} = 1000$ , with increasing  $t_{max}$  the outer envelope curve is completely filled.

**Right:** corresponding Poincaré section and two different close-ups as marked by rectangles in the second plot. The resolution is limited by the integration time (here  $t_{max} = 100000$ ).

Strange attractors

- resemble a puff pastry dough with self-similar structures
- are **fractal** objects with dimension  $1 < d_f < 2$  in the Poincaré section
- more than a line, less than an area, see chapter 2 for more about fractals

RunG

The Poincaré section defines a discrete sequence of the form

$$\begin{pmatrix} \phi(t_j) \\ \omega(t_j) \end{pmatrix} \rightarrow \begin{pmatrix} \phi(t_{j+1}) \\ \omega(t_{j+1}) \end{pmatrix} = \begin{pmatrix} \phi(t_j + 2\pi/\omega_D) \\ \omega(t_j + 2\pi/\omega_D) \end{pmatrix}$$

similar to the *Logistic Map* or the *Chirikov Map*. The iteration is, of course, more complicated and amounts to the numerical integration of the O.D.E.

**The bifurcation diagram** . . . is obtained by plotting the values of  $\phi$  or  $\omega$  that occur in the Poincaré section (after the initial phase) vs. the control parameter, e.g. for varying  $a$  with fixed  $r$ . It displays period doubling acc. to the Feigenbaum scenario as well as windows of periodic behavior and different routes to chaos.

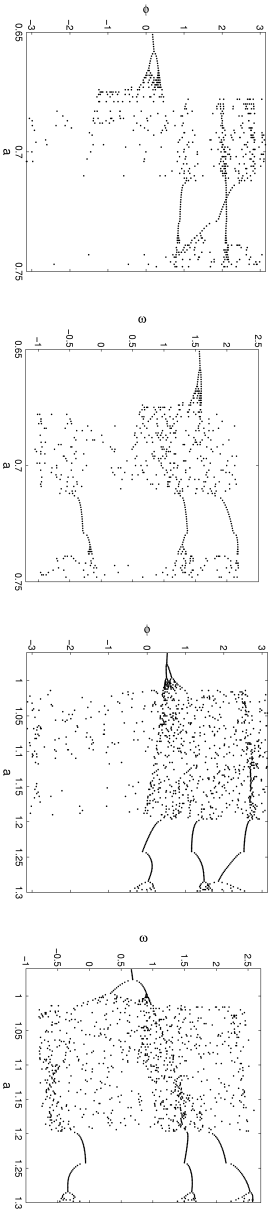


**Fig. 12:** Portions of the bifurcation diagrams of  $\phi$  (first, third) and  $\omega$  (second, fourth) vs.  $a$  for  $r = 0.25$ . The quality of the plots is limited by the resolution in  $a$  (0.002) and the number of recorded values (100) after the initial phase.

RunG

## Suggestions and remarks

- As in the Frenkel-Kontorova model (see assignment 1), chaotic motion emerges from the competition of different time or length scales. Here:
  - $\omega_o$ : frequency of the undisturbed oscillator
  - $\omega_D$ : frequency of the external torque
  - $1/r$ : time scale introduced by the damping
- suggestion: study the cases with  $\omega_D = \omega_o$  or  $\omega_D/\omega_o$  irrational
- other examples of chaotic systems:
  - non-linear mechanical systems: double pendulum, billiards, . . .
  - less simple systems: weather, stock market, ecological systems . . .
- Chaotic behavior is also relevant in quantum mechanical systems
- In principle, deterministic chaos is known since Poincaré. Computer simulations (models!) have made it feasible to study chaotic motion in detail and display it.
- Chaos (the *death of Laplace's demon*) is one of the foundations of Statistical Physics
- Additional literature (see also assignment 1)
  - G.L. Baker, J.P. Gallub, *Chaotic Dynamics*, Cambridge Univ. Press (1996)
  - H.-J. Jodl, H.J. Korsch, *Chaos: A Program Collection for PC*, Springer (1994)
  - E. Ott, *Chaos in Dynamical Systems*, Cambridge University Press (1993)
  - H.G. Schuster, *Deterministic Chaos: An Introduction*, VCH (1995)

RunG